the final results of this calculation agree with the experimental points to within about two per cent over the frequency range in which the calculations were performed. Further refinement is not warranted by the experimental data, and in any case a calculation from Hill's equation using a greater number of terms in the Fourier series for $F(z)$ becomes too difficult.

IV. Conclusions

From the agreement between the theoretical curve and the experimental points on Fig. 4 one can conclude that the analysis of these modulated surface-wave structures by means of a Mathieu equation is fairly accurate, in spite of the rather wide slots in these structures, the crudeness of the approximation to $F(z)$, and the fact that d and λ were of the same order of magnitude. One notes, as is to be expected, that the agreement is better in those cases where the modulation is less severe, but even where $F(z)$ varies over a four-to-one range, the result is not greatly in error.

Concerning the properties of modulated corrugated rods in general, one notes that v_p is more nearly independent of frequency than for a uniform rod, The tendency of v_p to decrease with decreasing wavelength is compensated by the fact that C_0 moves closer to the minimum of $F(z)$ as the form of $F(z)$ becomes more peaked. On the other hand, the effect of increasing the modulation, and hence C_1, for a given C_0, in the range of parameters used here is to decrease m, or increase v_p, but this is not universally true nor is it the dominant effect here. There is also very little difference between structures A and B with respect to dispersion.

Finally, with more extensive observation over the possible range of η and γ, one should be able to demonstrate the existence of the stop bands predicted in Fig. 6, but no such effect was observed in the experiments performed here.

Small Resonant Scatterers and Their Use for Field Measurements*

ROGER F. HARRINGTON†, MEMBER, IRE

Summary—**A general formulation for the back-scattered field from loaded objects is given. It is shown that small resonant objects produce a much greater back-scattered field than small nonresonant ones. The theory is applied to short dipoles and small loops. The use of small resonant scatterers to measure electric and magnetic fields by scattering techniques is discussed. Resonant scatterers are found to have several advantages over nonresonant scatterers when used for field measurements.**

I. Introduction

THE FIELD scattered by short straight wires has been used to measure microwave electric fields.[1–3] To separate the scattered field from the incident field more easily, the scattered field has been modulated by mechanical methods,[2] and by diodes.[3] Microwave magnetic fields have been measured by the field scattered from a small loop of wire, using two diodes such that they modulate the field due to the magnetic moment of the loop, but do not modulate the field due to the electric moment.[4] Scattering techniques for measuring electric and magnetic fields are attractive because no receiving equipment or transmission lines need be connected to the scatterer. This is in contrast to methods which detect the signal received by probes and loops; hence, scattering methods usually disturb the field to be measured less than do receiving methods.

This paper presents an analysis of small tuned scatterers, and proposes their use in scattering methods for measuring electric and magnetic fields. The use of resonant scatterers instead of nonresonant scatterers gives the following advantages: 1) The scattered field from resonant scatterers is much larger than that from nonresonant scatterers. Of the order of 30-db improvement can be obtained. 2) The magnetic moment of a loop scatterer can be greatly enhanced without materially changing the electric moment. This allows one to

* Received by the PGMTT, November 17, 1961; revised manuscript received, January 2, 1962. This study was supported by Rome Air Development Center, Rome, N. Y., under Contract No. AF 30(602)-1640.

† Department of Electrical Engineering, Syracuse University, Syracuse, N. Y.

[1] R. Justice and V. H. Rumsey, "Measurement of electric field distributions," IRE Trans. on Antennas and Propagation, vol. AP-3, pp. 177–180; October, 1955.

[2] A. Cullen and J. Parr, "A new perturbation method for measuring microwave fields in free space," *Proc. IEE*, vol. 102 B, pp. 836–844; November, 1955.

[3] J. H. Richmond, "A modulated scattering technique for measurement of field distributions," IRE Trans. on Microwave Theory and Techniques, vol. MTT-3, pp. 13–15; July, 1955.

[4] M. K. Hu, "On measurement of $\bar{E}$ and $\bar{H}$ field distributions by using modulated scattering methods," IRE Trans. on Microwave Theory and Techniques, vol. MTT-8, pp. 295–300; May, 1960.

use a tuned loop scatterer for most magnetic field measurements without the use of a complicated modulation scheme. 3) If modulation is desired, it can be accomplished in several ways not available for nonresonant scatterers. One can modulate the tuning reactance, or vary the scatterer size, or frequency modulate the field, as discussed in Section VIII. On the other hand, disadvantages of using resonant scatterers are: 1) tuning of the scatterer is required, and 2) construction of the tuned scatterer is more complicated than the untuned one.

II. General Theory

Fig. 1 represents the general problem of back scattering from a loaded scatterer. There are two objects, denoted by 1 and 2, each having a pair of closely-spaced terminals, also denoted by 1 and 2. Object 1, exited by a current source across terminals 1, produces an incident field. Object 2, loaded by an impedance Z_L across terminals 2, represents a loaded scatterer. The back-scattered voltage is defined as the difference between voltage appearing across terminals 1 when the scatterer (object 2 and Z_L) is present and when it is absent. The case of plane-wave back scattering is obtained when objects 1 and 2 are infinitely far apart. The general formulation of the problem is similar to that used by Professor Y. Y. Hu for loaded dipole scatterers.[5]

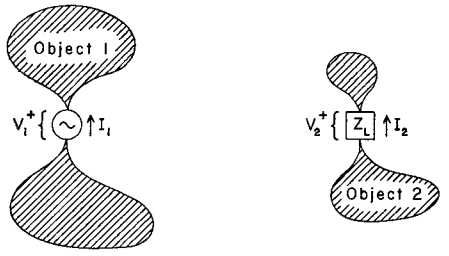

Fig. 1—The general case of back scattering by a loaded scatterer.

Terminal pairs 1 and 2 of Fig. 1 define a two-port network. For linear matter,

$$V_1 = Z_{11}I_1 + Z_{12}I_2$$
$$V_2 = Z_{21}I_1 + Z_{22}I_2, \tag{1}$$

where V_1, I_1 and V_2, I_2 are the voltages and currents at terminals 1 and 2, respectively. When all matter is isotropic, $Z_{12}=Z_{21}$. When the load impedance Z_L exists across terminals 2,

$$V_2 = -I_2Z_L. \tag{2}$$

Using (1) and (2), one finds the voltage at terminals 1 as

$$V_1 = \left(Z_{11} - \frac{Z_{12}^2}{Z_{22} + Z_L}\right)I_1. \tag{3}$$

Now define V_{10} as the voltage across terminals 1 when object 2 is absent and I_1 is impressed at terminals 1. Let the input impedance to this one-port network be denoted by

$$Z_1 = \frac{V_{10}}{I_1}. \tag{4}$$

Define the back-scattered voltage as the difference between the voltage at terminals 1 when object 2 is present and when it is absent, that is,

$$\Delta V = V_1 - V_{10}. \tag{5}$$

Then, using (3) and (4) in (5), one obtains

$$\Delta V = \left[(Z_{11} - Z_1) - \frac{Z_{12}^2}{Z_{22} + Z_L}\right]I_1. \tag{6}$$

Hence, the general problem of back scattering from a scatterer loaded by an arbitrary impedance Z_L involves the determination of three parameters: $(Z_{11}-Z_1)$, Z_{12} and Z_{22}.

Variational formulas for impedance parameters are well known.[6] Consider objects 1 and 2 to be perfectly conducting, and let

J_i = Current due to source I_i impressed at terminals i, the other terminals open circuited. (7)
$\boldsymbol{E}_i$ = Electric field due to J_i.

In general, $\boldsymbol{E}_i$ is related to the J_i by a tensor (or dyadic) Green's function Γ by

$$\boldsymbol{E}_i(r) = \int\int \Gamma(r, r') \cdot J_i(r')ds', \tag{8}$$

where r and r' denote radius vectors. A stationary formula for any of the impedance elements is then

$$Z_{ij} = \frac{-1}{I_iI_j}\int\int \boldsymbol{E}_i \cdot J_j ds. \tag{9}$$

The formula for Z_1 is the same as for Z_{11} except that object 2 is now absent. Defining

J_{10} = Current on object 1 due to I_1 when object 2 is absent, (10)
$\boldsymbol{E}_{10}$ = Electric field due to J_{10},

one has the stationary formula

$$Z_1 = \frac{-1}{I_1^2}\int\int \boldsymbol{E}_{10} \cdot J_{10} ds. \tag{11}$$

These formulas are applied to particular problems by assuming trial currents and calculating the desired impedances. Adjustable constants (variational parameters) can be included in the trial currents and evaluated by the Ritz procedure. A discussion of the evaluation of the Z's by the Ritz procedure is given in the Appendix.

[5] Y. Y. Hu, "Back-scattering cross section of a center-loaded cylindrical antenna," IRE Trans. on Antennas and Propagation, vol. AP-6, pp. 140–148; January, 1958.

[6] R. F. Harrington, "Time-Harmonic Electromagnetic Fields," McGraw-Hill Book Company, Inc., sect. 7–9; 1961.

Returning now to (6), one may note that the second term on the right-hand side is maximum when

$$Z_L = -j \operatorname{Im}(Z_{22}), \tag{12}$$

for passive Z_L. Eq. (12) will be used to define a *resonant scatterer*. When $(Z_{11}-Z_1)$ and Re (Z_{22}) are small, the scattered voltage is maximum at resonance. It follows a resonance curve when Z_L is tuned through resonance. Conducting scatterers small with respect to wavelength usually exhibit such resonance phenomena.

III. Plane-Wave Back Scattering

The general formulas can be specialized to plane-wave back scattering as follows. Let object 1 vanish so that terminals 1 are in empty space. The field of I_1 impressed across terminals 1 is then simply the field of a current element $I_1 l$ in free space. To be specific, let $I_1 l$ be z directed and located on the y axis a distance r from the origin, as shown in Fig. 2. As $r \to \infty$ one obtains in the vicinity of the origin a plane-wave field

$$\boldsymbol{E}_{10} = \boldsymbol{u}_z E_0 e^{-jky}, \tag{13}$$

where $\boldsymbol{u}_z$ = unit z-directed vector, k = wavenumber $(=2\pi/\lambda)$, and

$$E_0 = \frac{\eta I_1 l}{2\lambda r} e^{-jkr}, \tag{14}$$

where η = intrinsic impedance $(=\sqrt{\mu/\epsilon})$ and λ = wavelength.

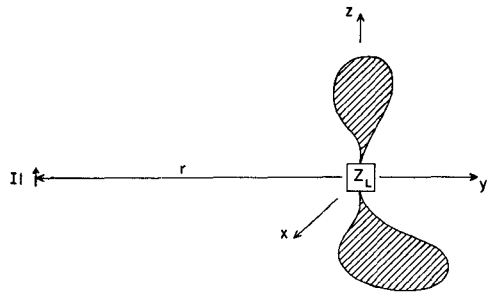

Fig. 2—Plane-wave back scattering is obtained by letting Il recede to infinity.

When the scatterer is present, the incident field induces a current on the scatterer, which in turn produces a scattered field $\boldsymbol{E}_s$. The component of $\boldsymbol{E}_s$ in the direction of $I_1 l$ at $I_1 l$ is called the *back-scattered field*. The area for which the incident field contains sufficient power to produce, by omnidirectional radiation, the same field as is back scattered by the scatterer, is called the *echo area* σ of the scatterer. In equation form

$$\sigma = \lim_{r\to\infty} 4\pi r^2 \left| \frac{\boldsymbol{u}_l \cdot \boldsymbol{E}_s}{E_0} \right|^2, \tag{15}$$

where $\boldsymbol{u}_l$ is a unit vector in the direction of $I_1 l$. In terms of the scattered voltage

$$\boldsymbol{u}_l \cdot \boldsymbol{E}_s = \Delta V / l, \tag{16}$$

and so the echo area is given by

$$\sigma = \lim_{r\to\infty} 4\pi \left(\frac{2\lambda}{\eta}\right)^2 \left(\frac{r}{l}\right)^4 \left| \frac{\Delta V}{I_1} \right|^2, \tag{17}$$

where ΔV is given by (6). The echo area is therefore of the form

$$\frac{\sigma}{\lambda^2} = \frac{1}{\pi} \left| A - \frac{B}{Z_{22} + Z_L} \right|^2, \tag{18}$$

where

$$A = \lim_{r\to\infty} \frac{4\pi}{\eta} \left(\frac{r}{l}\right)^2 (Z_{11} - Z_1),$$

$$B = \lim_{r\to\infty} \frac{4\pi}{\eta} \left(\frac{r}{l}\right)^2 Z_{12}^2. \tag{19}$$

The Z parameters can be obtained from (9) and (10) using (13) as the field from I_1. Note that $|A|^2/\pi$ is σ/λ^2 when $Z_L = \infty$, that is, when the scatterer terminals are open circuited. The scatterer is then unloaded, and one can use the known stationary formula[7]

$$(Z_{11} - Z_1) = \frac{\left(\iint \boldsymbol{E}_{10} \cdot \boldsymbol{J}_{12} ds \right)^2}{I_1^2 \iint \boldsymbol{E}_{12} \cdot \boldsymbol{J}_{12} ds}, \tag{20}$$

where $\boldsymbol{J}_{12}$ is the current on the open-circuited scatterer when it is excited by the incident plane wave, and $\boldsymbol{E}_{12}$ is the corresponding field.

An explicit formula for A is obtained by using (13), (14) and (20) in the first equation of (19). The result is

$$A = \frac{\eta}{4\pi} \frac{\left(k \iint e^{-jky} \boldsymbol{u}_z \cdot \boldsymbol{J}_{12} ds \right)^2}{\iint \boldsymbol{E}_{12} \cdot \boldsymbol{J}_{12} ds}, \tag{21}$$

which is still stationary. For a first-order approximation to B, one can assume $\boldsymbol{E}_1 = \boldsymbol{E}_{10}$ given by (13) and (14). Then from (9) and the first equation of (19) one obtains

$$B = \frac{\eta}{4\pi} \left(\frac{k}{I_2} \iint e^{-jky} \boldsymbol{u}_z \cdot \boldsymbol{J}_2 ds \right)^2, \tag{22}$$

where $\boldsymbol{J}_2$ is the current on the scatterer when excited by I_2 at its terminals. Procedures for obtaining higher-order approximations to B are discussed in the Appendix. Finally,

$$Z_{22} = \frac{-1}{I_2^2} \iint \boldsymbol{E}_2 \cdot \boldsymbol{J}_2 ds \tag{23}$$

[7] Harrington, *op. cit.*, sect. 7-10.

is the well-known stationary formula for the input impedance to the scatterer when viewed as a transmitting antenna.

The formulation of this section considers only linearly-polarized incident plane waves. The case of arbitrary polarization can be treated as the superposition of two linearly-polarized waves. The general procedure is given by Prof. Kouyoumjian.[8]

IV. Loaded Dipoles

The unloaded dipole has been analyzed by Prof. Tai,[9] and the loaded dipole by Prof. Hu.[5] Because Prof. Hu's results are difficult to specialize to short dipoles, and because it is desired to illustrate the application of the general formulas, the equations for short dipoles will be developed here.

Fig. 3 represents a short center-loaded dipole in a

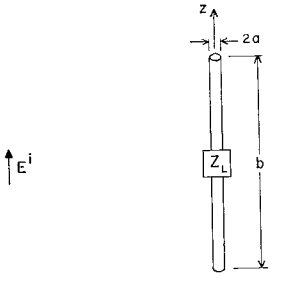

Fig. 3—A center-loaded dipole in a plane-wave field.

plane-wave field. When the dipole is excited by I_2 across its terminals the current can be approximated by

$$J_2 = u_z \frac{I_2}{2\pi a}\left(1 - \frac{2}{b}\,|\,z\,|\right), \tag{24}$$

where a is the wire radius and b the dipole length. This current can be considered to be a filament for calculating B; hence from (19)

$$B = \frac{\eta}{4\pi}\left[\frac{k}{I_2}\int_{-b/2}^{b/2} I_2\left(1 - \frac{2}{b}\,|\,z\,|\,\right)dz\right]^2 = \frac{\eta}{16\pi}(kb)^2. \tag{25}$$

The derivation of input impedance for dipole antennas can be found many places. For the current of (24), one can approximately evaluate (23) as

$$Z_{22} \approx \frac{\eta}{2\pi}\left[\frac{(kb)^2}{12} - j\frac{3\ln(2b/a) - 7}{kb}\right]. \tag{26}$$

When the dipole is open circuited and excited by the incident plane wave the current can be approximated by

$$J_{12} = u_z\left[\cos k\left(|\,z\,| - \frac{b}{4}\right) - \cos k\frac{b}{4}\right]. \tag{27}$$

The evaluation of (21) is then similar to the evaluation of (25) and (26), the result being

$$A \approx \frac{-j(kb)^3}{96[\ln(b/a) - 2]}. \tag{28}$$

The above evaluations give good accuracy for $kb < 1$. For longer dipoles one can use Professor Hu's results.[5]

Three special cases of interest are 1) the unloaded dipole, $Z_L = 0$, 2) the resonant dipole, satisfying (12), and 3) the open-circuited dipole, $Z_L = \infty$. For the short unloaded dipole, A is small compared to the second term of (18), and the first term of (26) is small compared to the second term. One then has

$$\frac{\sigma}{\lambda^2} \approx \frac{(kb)^6}{64\pi[3\ln(2b/a) - 7]^2}. \tag{29}$$

For resonance, Z_L should be an inductor adjusted according to (12); hence,

$$Z_L = j\omega L = j\frac{3\ln(2b/a) - 7}{kb}. \tag{30}$$

Now Z_L just cancels the second term of (26), and one has for the short resonant dipole

$$\frac{\sigma}{\lambda^2} \approx \frac{9}{4\pi} = 0.716. \tag{31}$$

Thus, the echo area of a small loss-free resonant dipole is independent of its physical size. This is analogous to the case of a small receiving dipole, which has an effective aperture independent of its physical size.[10] For actual dipoles, losses due to the finite resistivity of the conductor will substantially reduce the echo area of very small dipoles. This is condered in Section VII. When $Z_L = \infty$ (the open-circuited case), only the first term of (18) remains and

$$\frac{\sigma}{\lambda^2} \approx \frac{(kb)^6}{9216\pi[\ln(b/a) - 2]^2}. \tag{32}$$

This is the smallest possible echo area for a short dipole in the given orientation. For arbitrary orientations, all of the above echo areas should be multiplied by $\sin^4\theta$, where θ is the angle between the dipole axis and the E vector of the incident wave.

Fig. 4 illustrates the variation of echo area with frequency for dipoles of fixed dimensions. The case $b/a = 150$ is shown. Curve (a) is for an unloaded dipole, curve (b) is for a dipole continually tuned to resonance (Z_L is varied as λ is varied), curve (c) is for a dipole tuned to resonate when $b = \lambda/10$ by a fixed inductance L, and curve (d) is for an open-circuited dipole. The

[8] R. G. Kouyoumjian, "The back-scattering from a circular loop," *Appl. Sci. Research*, vol. 6, sec. B, no. 3, pp. 165–179; 1956.

[9] C. T. Tai, "Electromagnetic back-scattering from cylindrical wires," *J. Appl. Phys.*, vol. 23, pp. 909–916; August, 1952.

[10] J. D. Kraus, "Antennas," McGraw-Hill Book Company, Inc., New York, N. Y., p. 50; 1950.

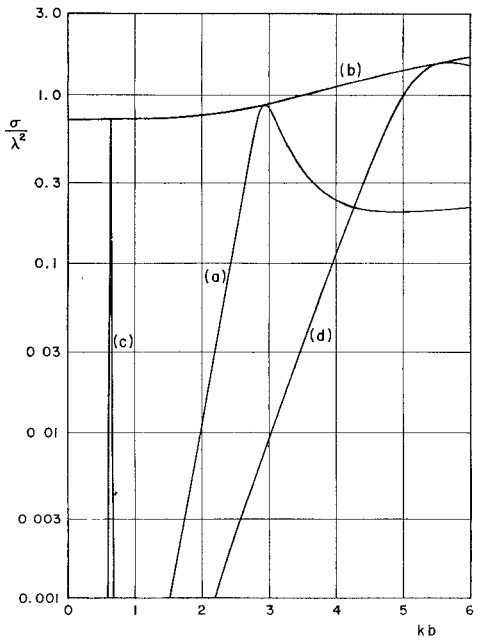

Fig. 4—Echo area of (a) unloaded dipole, (b) resonant dipole, (c) dipole resonated by fixed L, and (d) open-circuited dipole. $b/a = 150$.

numerical values were obtained from the above small-dipole formulas when $kb < 1$, and from Professor Hu's calculations when $kb > 1$.

Note that the input impedance to a short dipole, (26), is of the form of that for a series R-C circuit. When tuned by an inductance, the short dipole behaves similary to a series R-L-C circuit. Hence, resonance curves for short dipole scatterers are about the same as a series R-L-C resonance curve. A quality factor defined as

$$Q = \frac{|\operatorname{Im} Z_{22}|}{\operatorname{Re} Z_{22}} \tag{33}$$

has approximately the same relationship to the width of the echo area resonance curve as the Q of an R-L-C circuit has to the width of its power resonance curve. For short dipole scatterers

$$Q \approx 12 \frac{3 \ln (2b/a) - 7}{(kb)^3} \tag{34}$$

which illustrates how the Q increases as the dipole is made shorter. The Q of the loss-free $\lambda/10$ dipole of curve (c) of Fig. 4 is 485. Conductor losses will, of course, materially reduce the Q of very short dipoles. If a short loss-free dipole is resonated by a fixed inductance at a frequency ω_r, then at some other frequency ω in the vicinity of resonance

$$\frac{\sigma}{\lambda^2} = \frac{9}{4\pi}\left[1 + Q^2\left(\frac{\omega_r}{\omega}\right)^4\left(\frac{\omega_r}{\omega} - \frac{\omega}{\omega_r}\right)^2\right]^{-1}. \tag{35}$$

This result is obtained from (18) using (25), (26), (30), and neglecting A.

V. Loaded Loops

Unloaded wire loops in a plane-wave field have been analyzed by Professor Kouyoumjian.[8] A general analysis of loaded loops of arbitrary size has not yet appeared in the literature. An analysis of small loaded loops in a plane-wave field is given in this section.

Fig. 5 represents a small circular loop of wire, loaded by an impedance Z_L. When the loop is excited by a source I_2 across its terminals, the current is approximately uniform, that is,

$$\boldsymbol{I}_2 = I_2 \boldsymbol{u}_\phi, \tag{36}$$

where $\boldsymbol{u}_\phi$ is the unit ϕ-directed vector. From (22) one calculates

$$B = \frac{\eta}{4\pi}\left[\frac{k}{I_2}\int_0^{2\pi} e^{j(kd/2)\sin\phi}\boldsymbol{u}_z \cdot \boldsymbol{u}_\phi I_2 \frac{d}{2}\,d\phi\right]^2$$

$$\approx -\frac{\eta\pi}{64}(kd)^4. \tag{37}$$

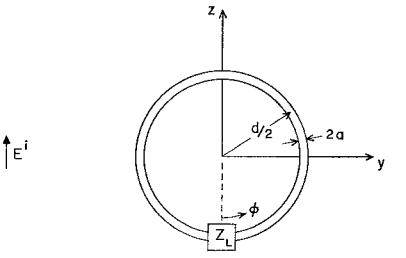

Fig. 5—A loaded loop in a plane-wave field.

The input resistance to a small loop with constant current is well-known and given by

$$\operatorname{Re}(Z_{22}) = \frac{\eta\pi}{96}(kd)^4. \tag{38}$$

The input reactance to a small loop is simply ωL where L is the low-frequency inductance; hence,

$$\operatorname{Im}(Z_{22}) = \eta k \frac{d}{2}\left[\ln\left(\frac{4d}{a}\right) - 2\right]. \tag{39}$$

When the loop is open circuited and excited by a plane wave, the current distribution depends markedly on the position of the loop terminals. When they are along the z axis, as shown in Fig. 5, the current can be approximated by

$$\boldsymbol{I}_{12} = \boldsymbol{u}_\phi \sin\phi. \tag{40}$$

One can then evaluate A according to (21). The result is

$$A = \frac{j\pi(kd)^3}{16[\ln(4d/a) - 2]}. \tag{41}$$

The assumed currents (36) and (40) are just the first two terms of the expansion used by Professor Kouyoum-

jian, and alternatively (37) and (41) could be abstracted from his small-loop formulas. The above formulas give reasonably accurate results when $kd<1$.

The three special cases 1) an unloaded loop, 2) a resonant loop and 3) an open circuited loop, will now be considered. For the unloaded loop, $Z_L=0$, (38) is small in magnitude compared to (39), and (26) reduces to

$$\frac{\sigma}{\lambda^2} \approx \frac{9\pi(kd)^6}{1024[\ln(4d/a) - 2]^2}. \tag{42}$$

This is identical to Professor Kouyoumjian's small loop result. For resonance, Z_L should be a capacitor adjusted according to (12); hence,

$$Z_L = \frac{1}{j\omega C} = \frac{\eta kd}{2j}\left[\ln\left(\frac{4d}{a}\right) - 2\right]. \tag{43}$$

Now Z_L cancels (39) and Z_{22} is given by (38). The first term of (18) is then negligible compared to the second term, and

$$\frac{\sigma}{\lambda^2} \approx \frac{9}{4\pi} = 0.716. \tag{44}$$

Note that this is identical to the echo area of the short resonant dipole (31). Again conductor losses will materially reduce σ for very small loops, as discussed in Section VII. When the loop is open circuited ($Z_L=\infty$), only the first term of (18) remains and

$$\frac{\sigma}{\lambda^2} \approx \frac{\pi(kd)^6}{256[\ln(4d/a) - 2]^2}. \tag{45}$$

The open-circuit echo area is sensitive to the position of the loop terminals, but it is always smaller than the short-circuit echo area (42) for small loops. When the loop of Fig. 5 is rotated about the z axis through an angle θ, the parameter B, (37), should be multiplied by $\sin^2\theta$. This results in (44) being multiplied by $\sin^4\theta$, and (42) multiplied by $(2+\sin^2\theta)^2/9$. Eq. (45) is unchanged.

Fig. 6 shows the variation of echo area with frequency for loops of dimensions $d/a=200$. Curve (a) is for an unloaded loop, curve (b) is for a loop continuously tuned to resonance, curve (c) is for a loop tuned to resonate when $d=\lambda/10$ by a fixed capacitance C, and curve (d) is for an open-circuited loop. These curves are only approximate because calculations for the general loaded loop are not available. For $kd<1$, the small loop formulas can be used. Some points on the unloaded-loop curve were abstracted from Professor Kouyoumjian's calculations.

Just as for the short dipole, the small loop behaves similarly to a series R-L-C circuit. The quality factor is again defined by (33), which, for small wire loops, becomes

$$Q \approx \frac{48}{\pi}\frac{\ln(4d/a) - 2}{(kd)^3}. \tag{46}$$

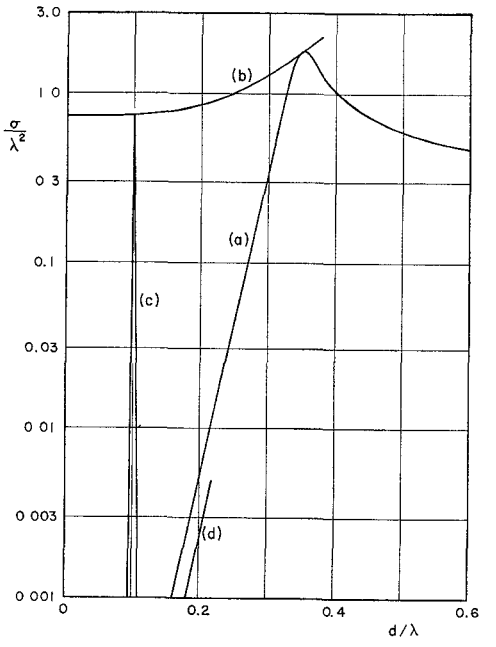

Fig. 6—Echo areas of (a) unloaded loop, (b) resonant loop, (c) loop resonated by fixed C, and (d) open-circuited loop. $d/a=200$.

The Q of the loss-free $\lambda/10$ loop (curve (c) of Fig. 6) is 292. This would be reduced by conductor losses for an actual loop. If a small loss-free loop is resonated by a fixed capacitance at a frequency ω_r, then at some other frequency ω in the vicinity of resonance

$$\frac{\sigma}{\lambda^2} = \frac{9}{4\pi}\left[1 + Q^2\left(\frac{\omega_r}{\omega}\right)^8\left(\frac{\omega}{\omega_r} - \frac{\omega_r}{\omega}\right)^2\right]^{-1}. \tag{47}$$

This equation is obtained from (18) using (37)–(39), (46) and neglecting A.

VI. Small Scatterers in an Arbitrary Field

For the general problem of back scattering, Fig. 1, the back-scattered voltage is always given by (6). In general, the presence of the scatterer (object 2) modifies the current on the originally excited object (object 1), and vice versa. The Appendix considers the complete formulation of the problem taking into account this proximity effect. For this section it is assumed that the scatterer is small enough and far enough from object 1 to neglect such interaction. In other words, it is assumed that the source of the field to be measured is not materially changed by the introduction of the scatterer. Then $Z_{11}\approx Z_1$, and the first term of (6) is small. When the scatterer is small and resonant, $(Z_{11}-Z_1)$ is negligible compared to the second term of (6). [For example, compare curves (c) with (d) in Figs. 4 and 6.] Furthermore, Z_{22} is a characteristic of the scatterer alone. Hence, when the proximity effect is neglected, only the parameter

$$Z_{12} = \frac{-1}{I_1 I_2}\iint \boldsymbol{E}_1 \cdot \boldsymbol{J}_2 ds \tag{48}$$

depends upon the field into which the scatterer is placed.

Let $\boldsymbol{r}=\boldsymbol{u}_x x+\boldsymbol{u}_y y+\boldsymbol{u}_z z$ denote the radius vector from the coordinate origin (chosen at the midpoint of the scatterer) to a field point. Let $\boldsymbol{E}(\boldsymbol{r})=\boldsymbol{E}_2(x, y, z)$ denote the field into which the scatterer is introduced. Then, in the vicinity of the origin, $\boldsymbol{E}$ can be expanded in the Taylor series

$$\boldsymbol{E}(\boldsymbol{r}) = \boldsymbol{E}(0) + (\boldsymbol{r}\cdot\nabla)\boldsymbol{E}(0) + \cdots, \tag{49}$$

where the notation $(\boldsymbol{r}\cdot\nabla)\boldsymbol{E}(0)$ means that $\boldsymbol{r}$ is set equal to zero after differentiation in $\boldsymbol{E}$, but not in $\boldsymbol{r}$. The higher order terms of the expansion can be neglected if $\boldsymbol{r}$ is small enough.

Consider first the small tuned dipole scatterer, Fig. 3. Let $I(z)$ denote the current on the dipole when it is excited by $I_2=I(0)$ at its terminals. Then

$$Z_{12} = \frac{-1}{I_1 I_2}\int_{-b/2}^{b/2} I\boldsymbol{u}_z\cdot\boldsymbol{E}dz, \tag{50}$$

where $\boldsymbol{E}$ is given by (49) with $\boldsymbol{r}=\boldsymbol{u}_z z$. For small b, one has

$$Z_{12} \approx \frac{-1}{I_1 I_2}\int_{-b/2}^{b/2} I\left[E_z(0) + z\frac{\partial E_z(0)}{\partial z}\right]dz. \tag{51}$$

If the dipole terminals are centered, $I(z)$ is an even function of z, and the first term of the integrand is odd. Then

$$Z_{12} \approx \frac{-1}{I_1 I_2}E_z(0)\int_{-b/2}^{b/2} Idz = \frac{-p_2}{I_1 I_2}E_z(0), \tag{52}$$

where p_2 is the current moment of the dipole. Hence, Z_{12} is proportional to $E_z(0)$, and ΔV is proportional to $E_z^2(0)$. The scattered voltage due to a small dipole in an arbitrary field is therefore proportional to the square of the component of $\boldsymbol{E}$ along the wire, and the dipole scatterer can be used to measure electric fields. Note that this is true for a tuned dipole only if it is center loaded, else the second term of (51) does not vanish.

Now let the scatterer be a small tuned loop, such as shown in Fig. 5. When excited by I_2 the loop current is approximately uniform. Hence

$$Z_{12} \approx \frac{-1}{I_1 I_2}\oint I_2\boldsymbol{E}\cdot d\boldsymbol{l}, \tag{53}$$

where the integral is taken once around the loop. Using (49) in (53), one has for small $\boldsymbol{r}$

$$Z_{12} \approx \frac{-1}{I_1}\oint [\boldsymbol{E}(0) + (\boldsymbol{r}\cdot\nabla)\boldsymbol{E}(0)]\cdot d\boldsymbol{l}. \tag{54}$$

The first term integrates to zero. To evaluate the second term, let the loop (planar, but not necessarily circular) lie in the $z=0$ plane. Then $d\boldsymbol{l}=\boldsymbol{u}_x dx+\boldsymbol{u}_y dy$ and

$$Z_{12} \approx \frac{-1}{I_1}\left[\frac{\partial E_x(0)}{\partial x}\oint xdx + \frac{\partial E_x(0)}{\partial y}\oint ydy + \frac{\partial E_y(0)}{\partial x}\oint xdy + \frac{\partial E_y(0)}{\partial y}\oint ydy\right]. \tag{55}$$

The integrals are

$$\oint xdx = \oint ydy = 0 \tag{56}$$

$$\oint xdy = -\oint ydx = S, \tag{57}$$

where S is the area of the loop. Eq. (55) then becomes

$$Z_{12} \approx \frac{-1}{I_1}S\left(\frac{\partial E_y}{\partial x} - \frac{\partial E_x}{\partial y}\right) = \frac{j\omega}{I_1}SB_z \tag{58}$$

or, putting it into a form independent of the choice of coordinates

$$Z_{12} \approx \frac{j\omega}{I_1}\boldsymbol{S}\cdot\boldsymbol{B}(0), \tag{59}$$

where $\boldsymbol{S}$ is the vector area of the loop. Thus, Z_{12} is proportional to the component of $\boldsymbol{B}$ in the direction of the loop moment (perpendicular to the loop area). For example, for the loop of Fig. 5, $\boldsymbol{S}=(\pi/4)d^2\boldsymbol{u}_x$, and Z_{12} is proportional to B_x. Hence, the scattered voltage due to a small resonant loop is proportional to the square of the component of $\boldsymbol{B}$ perpendicular to the loop, and the scatterer can be used to measure magnetic fields. This result is valid for loops of arbitrary shape. It is not valid for untuned loops, because the first term of (6) is then of the same order of magnitude as the second term. Even for resonant loops, if $\boldsymbol{E}$ were very large and $\boldsymbol{B}$ very small at some point in space, the scattered voltage would no longer be a measure of $\boldsymbol{B}$ because the first term of (6) might be appreciable.

VII. Effect of Wire Resistance

The effect on echo area and back scattering due to the finite conductivity of wires easily can be incorporated into the previous solutions. Assume that the wire has sufficiently high conductivity that 1) the current distribution on the scatterer is not materially changed from that on a perfect conductor, and 2) the resistance per unit length R of the wire can be approximated by the surface resistivity divided by the circumference of the wire. Then, for nonmagnetic conductors,

$$R = \frac{1}{2\pi a}\sqrt{\frac{\omega\mu}{2\sigma}} = \frac{1}{a}\sqrt{\frac{30}{\sigma\lambda}}, \tag{60}$$

where a = wire radius and σ = conductivity of the wire. In most small scatterer applications the first term of (6) is negligible compared to the second, and Z_{12} depends

only on the current distribution. Hence, the only significant change introduced by wires of finite conductivity occurs in the calculation of Z_{22}. This change can be accounted for by adding an I^2R loss to the previously derived radiation impedance. Hence,

$$Z_{22} = R_{\text{loss}} + Z_{22}^0, \tag{61}$$

where Z_{22}^0 is the loss-free radiation impedance given by (23). For wire scatterers,

$$R_{\text{loss}} \approx \frac{1}{I_2^2} \int_{\text{wire}} I^2 R dl. \tag{62}$$

However, when the scatterer is loaded, there is an additional loss in the loading impedance

$$Z_L = R_L + jX_L. \tag{63}$$

For resonant dipoles, this R_L of the resonating inductor is more important than R_{loss} in limiting the backscattered field from short dipoles.

For example, for a short dipole scatterer, the current is given by (24) and

$$R_{\text{loss}} = \frac{1}{I_2^2} \int_{-b/2}^{b/2} I_2^2 \left(1 - \frac{2}{b} |z|\right)^2 R dz$$
$$= \frac{1}{3} Rb = \frac{b}{3a} \sqrt{\frac{30}{\sigma\lambda}}. \tag{64}$$

For a copper dipole ($\sigma = 5.7 \times 10^7$) with $b/a = 150$, operating at $\lambda = 0.1$ m, one has $R_{\text{loss}} = 0.12$ ohm. If the dipole is $b = \lambda/10$ in length, then from (6) one finds Re $(Z_{22}^0) = 2$ ohms. This is much larger than the loss resistance. However, one needs a resonating inductor. If the inductor is constructed of the same wire as the dipole, the wire will be of the order of $\lambda/2$ in total length. It then has a resistance of

$$R_L \approx R(\lambda/2) = 1.8 \text{ ohms}, \tag{65}$$

which is approximately equal to the radiation resistance. The Q of the scatterer plus Z_L is then approximately half of the 485 unloaded Q calculated in Section IV, or $Q \approx 250$. This will reduce the echo area by about 3 db over what it was in the loss-free case. In general, for short resonant dipole scatterers

$$\frac{1}{Q} \approx \frac{1}{Q_0} + \frac{1}{Q_L}, \tag{66}$$

where Q_0 is the loss-free Q of the dipole, given by (34), and Q_L is the Q of the resonating inductance.

For the wire loop, the terminating impedance is a capacitor, which is usually high Q. Then the principal losses are those of the loop, given by

$$R_{\text{loss}} = R(\pi d) = \pi \frac{d}{a} \sqrt{\frac{30}{\sigma\lambda}}. \tag{67}$$

For example, taking a copper wire loop having $d/a = 200$ and $\lambda = 0.1$ m, one calculates $R_{\text{loss}} = 1.45$ ohms. Considering the loop to be $d = \lambda/10$ in diameter, from (38) one has Re $(Z_{22}^0) = 1.9$ ohms. In this case the loss resistance is of the same order of magnitude as the radiation resistance, and the Q is reduced from 292 in the nonlossy case to $Q = 165$ in the lossy case. Neglecting losses in the resonating capacitor, one has in general for small resonant loops

$$\frac{1}{Q} = \frac{1}{Q_0}\left[1 + \frac{R_{\text{loss}}}{\text{Re } (Z_{22}^0)}\right], \tag{68}$$

where Q_0 is the loss-free Q, given by (46), and Re (Z_{22}^0) is given by (38).

VIII. Tuning and Modulation

The use of resonant scatterers for field measurements requires some sort of tuning procedure. There are basically three ways that this might be accomplished: 1) the load impedance Z_L can be varied, 2) the dimensions or geometry of the scatterer can be varied, and 3) the frequency of the field can be varied. At the longer wavelengths, say of the order of several meters, ordinary variable inductors and capacitors can be used for tuning according to method 1). As the wavelength is made shorter, the construction of variable reactors becomes more difficult, and method 2) becomes attractive. For example, consider the scatterer of Fig. 7(a).

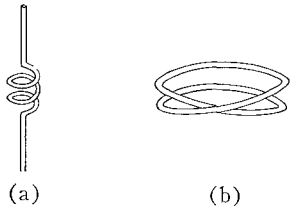

(a) (b)

Fig. 7—Small resonant scatterers. (a) Dipole. (b) Two-turn loop

It consists of a piece of wire of length a little less than $\lambda/2$, with the central portion wound in a loosely-spaced coil. If one stretches the dipole in the axial direction, the capacitive reactance of the dipole changes rapidly [see (26)] while the inductive reactance of the coil changes very little. Hence, the dipole can be tuned by small adjustments of its length. Similarly, Fig. 7(b) shows a loop scatterer that can be tuned by compressing it. The loop consists of two or more loosely-spaced turns of wire with the two ends connected together. The total length of wire is a little more than one wavelength. (Hence, for a two turn loop, $d \approx \lambda/6$; for a three turn loop, $d \approx \lambda/9$.) As the loop is squeezed closer together (in the axial direction), the coupling between adjacent wires increases and the loop resonates at shorter wavelengths. Finally, if it is desired that scatterers of fixed dimensions and loads be used, the signal frequency can be varied [method 3)]. In this case one constructs a

scatterer to resonate at approximately the desired frequency, and then the signal oscillator is tuned.

It is easier to separate the scattered signal from the incident field if the former is modulated and the latter not modulated. For this reason diode loads with a modulated bias have been used with untuned dipole and loop scatterers.[3,4] Mechanical rotation of unloaded dipoles has also been used to obtain modulation of the scattered signal.[2] These methods of modulation can continue to be used with resonant scatterers. However, some alternative modulation methods can be used with resonant scatterers that cannot be used with nonresonant ones. Because the resonant scatterers are high Q, small changes in either 1) the tuning reactance, or 2) the scatterer dimensions, or 3) the signal frequency can produce large changes in the scattered field. To utilize possibility 1), one could either mechanically or electrically modulate the tuning reactance. For 2), a vibration of the scatterer could be used to modulate the scattered signal. The scatterer might be made mechanically resonant at the desired modulation frequency, as well as electrically resonant at the signal frequency. Then the desired mechanical vibration could be obtained from a sound wave impinging upon the scatterer. Finally, to utilize method 3) the original signal frequency could be frequency modulated. The scattered signal would then be amplitude modulated. Only a small frequency deviation, of the order of $1/Q$ of the scatterer, would be needed for the frequency modulation of the signal generator. Note also that the modulation frequency of the scattered amplitude-modulated signal from the scatterer would be twice the modulation frequency of the original frequency-modulated signal, if the center frequency is the resonant frequency of the scatterer. To take full advantage of this difference between the scattered signal and the incident signal, special detection circuits can be devised. For example, an AM detector having a tuning Q large compared to the Q of the scatterer, and $1/Q$ small compared to the frequency deviation, can be used. This assumes that the scatterer is the only high Q object resonating at the test frequency.

Appendix

A Formulation of the General Two-Port Problem

The two-port problem of Fig. 1 can be viewed as a pair of coupled antennas. Profs. Hu and Hu have considered the general variational solution for a system of N coupled linear antennas.[11] Their analysis is actually applicable to a general N-port system of conducting bodies if one makes the following simple changes. Replace all scalar Green's functions by tensor Green's functions, all filaments of currents by surface currents, and all line integrals by surface integrals.

Combining (9) and (10) of Section II one has the variational formula

$$Z_{ij} = \frac{-1}{I_i I_j} \int\int ds' \int\int ds J_i(\boldsymbol{r}) \cdot \Gamma(\boldsymbol{r}, \boldsymbol{r}') \cdot J_j(\boldsymbol{r}') = \frac{-1}{I_i I_j} (J_i, J_j). \tag{69}$$

The last equality defines the scalar product (J_i, J_j). In general, J_i consists of current induced on object i by I_i, denoted by J_{ii}, plus current induced on object j by I_i, denoted by J_{ij}; hence,

$$J_1 = J_{11} + J_{12} \qquad J_2 = J_{22} + J_{21}. \tag{70}$$

Following Professors Hu, one assumes trial currents of the form

$$\begin{aligned} J_{11} &= \hat{J}_0 + a_1\hat{J}_1 + a_2\hat{J}_2 + \cdots + a_M\hat{J}_M \\ J_{12} &= a_{M+1}\hat{J}_{M+1} + \cdots + a_N\hat{J}_N \\ J_{21} &= b_1\hat{I}_1 + b_2\hat{I}_2 + \cdots + b_M\hat{I}_M \\ J_{22} &= \hat{I}_0 + b_{M+1}\hat{I}_{M+1} + \cdots + b_N\hat{I}_N \end{aligned} \tag{71}$$

where the a_n and b_n are variational parameters, and the vector currents $\hat{J}_n$ and $\hat{I}_n$ satisfy

$$\hat{J}_n = \hat{I}_n = 0 \qquad \text{at terminals 1 and 2} \tag{72}$$

if $n \neq 0$, and

$$I_1 = \oint \hat{J}_0 \cdot \boldsymbol{n} \times dl \qquad I_2 = \oint \hat{I}_0 \cdot \boldsymbol{n} \times dl, \tag{73}$$

where these integrals are taken around terminals 1 and 2, respectively. In other words, the entire excitation currents I_1 and I_2 are obtained from $\hat{J}_0$ and $\hat{I}_0$, and all other trial currents are zero at the terminals. Professors Hu show that one should choose the number of variational parameters a_n equal to the number of b_n, since the order of approximation corresponds to the smallest number of a_n or b_n. It is also shown below that there should be as many variational parameters in J_{ij} as in J_{jj}, else the solution for Z_{12} will diverge as the objects are moved farther apart. In other words, M and N should be the same numbers in J_1 and J_2, as is shown in (71).

Substitution of (70) and (71) into (69), and setting $\partial Z_{ij}/\partial a_n = \partial Z_{ij}/\partial b_n = 0$ for all n, yields the following formulas.[11] For Z_{12} one has either

$$Z_{12} = (\hat{I}_0, \hat{J}_0) - \begin{bmatrix} (\hat{I}_0, \hat{J}_1) & (\hat{I}_0, \hat{J}_2) & \cdots & (\hat{I}_0, \hat{J}_N) \end{bmatrix} \begin{bmatrix} (\hat{I}_1, \hat{J}_1) & (\hat{I}_1, \hat{J}_2) & \cdots & (\hat{I}_1, \hat{J}_N) \\ (\hat{I}_2, \hat{J}_1) & (\hat{I}_2, \hat{J}_2) & \cdots & (\hat{I}_2, \hat{J}_N) \\ \cdots & \cdots & \cdots & \cdots \\ (\hat{I}_N, \hat{J}_1) & (\hat{I}_N, \hat{J}_2) & \cdots & (\hat{I}_N, \hat{J}_N) \end{bmatrix}^{-1} \begin{bmatrix} (\hat{I}_1, \hat{J}_0) \\ (\hat{I}_2, \hat{J}_0) \\ \cdots \\ (\hat{I}_N, \hat{J}_0) \end{bmatrix} \tag{74}$$

[11] M. K. Hu and Y. Y. Hu, "Successive variational approximations of impedance parameters in a coupled antenna system," IRE Trans. on Antennas and Propagation, vol. AP-7, pp. 373–379; October, 1959.

or alternatively,

$$Z_{12} = \frac{\begin{vmatrix} (\hat{I}_0, \hat{J}_0) & (\hat{I}_0, \hat{J}_1) \cdots (\hat{I}_0, \hat{J}_N) \\ (\hat{I}_1, \hat{J}_0) & (\hat{I}_1, \hat{J}_1) \cdots (\hat{I}_1, \hat{J}_N) \\ \cdots & \cdots \\ (\hat{I}_N, \hat{J}_0) & (\hat{I}_N, \hat{J}_1) \cdots (\hat{I}_N, \hat{J}_N) \end{vmatrix}}{\begin{vmatrix} (\hat{I}_1, \hat{J}_1) \cdots (\hat{I}_1, \hat{J}_N) \\ \cdots \\ (\hat{I}_N, \hat{J}_1) \cdots (\hat{I}_N, \hat{J}_N) \end{vmatrix}}, \tag{75}$$

where the scalar products $(\hat{I}_m, \hat{J}_n)$ are as defined by (69). Formulas for Z_{11} are (74) and (75) with all $\hat{I}_n$'s replaced by the corresponding $\hat{J}_n$'s. Formulas for Z_{22} are (74) and (75) with all $\hat{J}_n$'s replaced by the corresponding $\hat{I}_n$'s.

To illustrate the difficulty that occurs if J_{ij} does not have the same number of variational parameters as J_{ij}, suppose

$$\begin{aligned} J_{11} &= \hat{J}_0 \qquad J_{12} = a_1\hat{J}_1, \\ J_{22} &= \hat{I}_0 \qquad J_{21} = b_1\hat{I}_1. \end{aligned} \tag{76}$$

[This choice was purposely excluded by (71).] The mutual impedance (74) or (75) then becomes

$$Z_{12} = (\hat{I}_0, \hat{J}_0) - \frac{(\hat{I}_0, \hat{J}_1)(\hat{I}_1, \hat{J}_0)}{(\hat{I}_1, \hat{J}_1)}. \tag{77}$$

As the two objects are separated

$$(\hat{I}_0, \hat{J}_0) \to 0 \qquad (\hat{I}_1, \hat{J}_1) \to 0, \tag{78}$$

because these products involve currents on different objects, and

$$(\hat{I}_0, \hat{J}_1) \to C_{01} \qquad (\hat{I}_1, \hat{J}_0) \to C_{10} \tag{79}$$

(C's denote constants) because they involve currents on the same object. Hence, as the two objects are separated, by (77) one has $Z_{12} \to \infty$, an impossibility. This absurd result can be explained by noting that

$$a_1 = -\frac{(\hat{I}_1, \hat{J}_0)}{(\hat{I}_1, \hat{J}_1)} \to \infty \tag{80}$$

in the variational solution, and, hence, no value of a_1 can improve the solution. The parameter b_1 behaves similarly. One can view this as a poor choice of trial functions. However, if J_{12} is chosen to have the same number of variational parameters as J_{22}, and similarly for J_{12} and J_{11}, as required by (71), then the difficulty does not arise. To show this, note that, as the objects are separated, the denominator of (75) becomes of the form

$$\left|\begin{array}{c|c} \text{constants} & 0\text{'s} \\ \hline 0\text{'s} & \text{constants} \end{array}\right| \tag{81}$$

which is finite. If J_{ij} does not have the same number of variational parameters as J_{jj}, then one or more rows or columns of zeros appear in the "constants" sections of (81), and the denominator of (75) vanishes as the objects are separated. Of course, no such difficulty arises in the calculation of Z_{11} and Z_{22}.

Wide-Band Matching of Lossless Waveguide Two-Ports*

DARKO KAJFEŽ†

Summary—**A new procedure of matching is presented, based in the equations which transform the output reflection coefficient of a lossless two-port network into the input reflection coefficient. The parameters of the equations are the residual reflection coefficients which can be easily measured. The optimum reflection coefficients which have the minimum frequency variation are computed for the specific case when the frequency variation of the residual reflection coefficients can be approximated by a circular arc in the Smith diagram. An illustrative example is given to explain the determination of the position and the size of the inductive obstacles that match a waveguide two-port structure within a wide frequency band.**

* Received by the PGMTT, October 17, 1961; revised manuscript received, January 2, 1962.

† Institute for Automation, Ljubljana, Yugoslavia.

I. Introduction

THERE ARE a considerable number of waveguide structures that can be represented by an equivalent two-port network. Waveguide bends, rotary joints, coaxial-to-waveguide transducers and many other waveguide components are typical examples of lossless two-port waveguide structures. Frequently these components are not completely matched and, in spite of careful design, they produce a discontinuity in the waveguide system. The aim of this article is to present a method that will make it possible to match the residual reflections of a two-port wave-